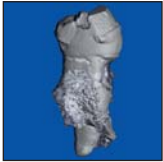


Three-dimensional Micro-computed Tomographic Evaluation of Periodontal Regeneration: A Human Report of Intrabony Defects Treated with Bio-Oss Collagen



Marc L. Nevins, DDS, MMSc*
 Marcelo Camelo, DDS**
 Alberto Rebaudi, MD, DDS***
 Samuel E. Lynch, DMD, DMSc****
 Myron Nevins, DDS*****

This study utilized three-dimensional micro-computed tomography (micro-CT) to evaluate the regenerative response to Bio-Oss Collagen when used alone or in combination with a Bio-Gide bilayer collagen membrane for the treatment of four intrabony defects (5 to 7 mm) around single-rooted teeth. The micro-CT observations are compared to the clinical, radiographic, and histologic results, which have been previously reported. After reflecting a full-thickness flap, thorough degranulation and root planing were accomplished. Bio-Oss Collagen was then used to fill the defects, and in two cases a Bio-Gide membrane was placed over the filled defect. Radiographs, clinical probing depths, and attachment levels were obtained before treatment and immediately preceding en bloc resection of teeth and surrounding tissues 9 months later. A mean pocket depth reduction of 5.75 mm and mean clinical attachment level gain of 5.25 mm were recorded. The histologic evaluation demonstrated the formation of a complete new attachment apparatus with new cementum, periodontal ligament, and alveolar bone at the level of and coronal to the calculus reference notch. Micro-CT evaluation confirmed the histologic results and demonstrated the absence of ankylosis or root resorption for all specimens. This human histologic study demonstrated that Bio-Oss Collagen has the capacity to facilitate regeneration of the periodontal attachment apparatus when placed in intrabony defects. Micro-CT observations confirmed the histologic results and enhanced the three-dimensional understanding of periodontal wound healing. The results indicate that micro-CT may be useful for three-dimensional evaluation of periodontal regenerative procedures. (Int J Periodontics Restorative Dent 2005;25:365–373.)

*Clinical Instructor, Department of Periodontology, Harvard School of Dental Medicine, Cambridge, Massachusetts; and Private Practice, Boston, Massachusetts.

**Director, Brazil Institute for Advanced Dental Studies, Belo Horizonte, Brazil.

***Private Practice, Genova, Italy; and Vice President of BioCRA, Biomaterials Clinical Research Association, Pescara, Italy.

****Clinical Professor, Vanderbilt University, Nashville, Tennessee; and President, BioMimetic Pharmaceuticals, Franklin, Tennessee.

*****Clinical Associate Professor of Periodontology, Harvard School of Dental Medicine, Cambridge, Massachusetts; and Private Practice, Swampscott, Massachusetts.

Correspondence to: Dr Marc Nevins, 175 Cambridge Street, Suite 310, Boston, MA 02114.
 E-mail: marc_nevins@hms.harvard.edu

Histologic evidence of new cementum, periodontal ligament (PDL), and alveolar bone adjacent to a previously diseased root surface notched at the apical extent of calculus is the only current methodology available to demonstrate periodontal regeneration.^{1,2} Biomaterials proposed for use as periodontal regenerative materials must demonstrate clear histologic evidence of regeneration to satisfy this definition. Obtaining specimens for human histologic studies is difficult, however, and has led to limited information, obtained primarily from two randomized controlled trials and multiple case studies.^{3–8} Surrogate measures of periodontal regeneration have included re-entry surgery, bone sounding, radiographic evaluation, and clinical attachment and probing depth measurements. Unfortunately, none of these alternatives can differentiate between repair and regeneration of the periodontal structures.^{9,10}

In the future it would be beneficial to have a method to provide three-dimensional analysis of periodontal regeneration as an alternative to histologic evaluation with biopsy specimens. Current histologic techniques utilize hard tissue

histologic methodology to prevent artifacts that distort the integrity of the tissues but limit the number of sections available (2 to 3 sections per specimen). Demineralized tissue preparation, on the other hand, provides stepped serial sections but frequently results in damage to the specimen, which challenges histologic interpretation.

In 1989, Feldkamp et al introduced a micro-computed tomographic (micro-CT) system that could create three-dimensional (3D) images with a resolution of 50 μm .¹¹ More recent developments provide higher-resolution 3D images and quantitative measurements of the trabecular bone structure.^{12,13} These recent technical advances provide the opportunity to study bone biopsies with 3D micro-CT. Three-dimensional micro-CT scanning procedures have been proposed as an alternative approach to evaluate and quantify bone in three dimensions and have been validated as a method to provide 3D analysis of cancellous bone.^{9,14,15} Micro-CT analysis explores not only the quantity of bone present but can demonstrate the orientation of individual bone trabeculae in three dimensions.

The aim of the present pilot study was to use micro-CT to analyze the 3D morphology of bone and the dimensions of the PDL to determine the ability of a mineralized collagen bone substitute (Bio-Oss Collagen, Osteohealth) to achieve regeneration in human intrabony periodontal defects.

Methods and materials

Four single-rooted teeth with advanced periodontal disease and judged to have a hopeless prognosis were selected for the study. Appropriate radiographs, probing depths, and attachment levels were obtained prior to surgery. Informed consent was received from all four patients.

The surgical procedures for the present study have been previously reported and will be summarized here.¹⁶ Reversed-bevel incision, full-thickness flaps were reflected to provide access to degranulate the bony defects. The root surfaces were notched with a half-round bur at the apical extent of the calculus. The root surfaces were then aggressively scaled, root planed, and treated with topical application of tetracycline paste for 4 minutes to achieve demineralization and decontamination. After the root surfaces were thoroughly rinsed, osseous walls of the defects that appeared sclerotic were perforated with a small round bur or hand instruments to encourage bleeding. The defects were then filled with mineral collagen bone substitute to the level of the osseous crest. Two of the four defects were then covered with a bilayer collagen membrane Bio-Gide, (Osteohealth) that had been trimmed and adapted to cover the filled defect. The remaining two defects had an additional layer of the mineral collagen bone substitute placed in similar fashion to a barrier membrane. The soft tissue flaps were then sutured with Gore-Tex (W.L. Gore) or

polypropylene sutures to achieve primary closure. A periodontal dressing (CoePak, GC America Inc) was placed and then replaced after 7 days. Sutures were removed after 14 days. Patients received penicillin VK (1 g/d for 7 days) and were instructed to rinse with chlorhexidine digluconate twice daily for 8 weeks. Postsurgical examination and supragingival cleansing of the surgical site occurred at 7, 14, and 21 days. Oral hygiene assessments and supragingival scaling were performed after 4, 6, and 8 weeks and monthly thereafter until the time of biopsy, at 9 months.

Clinical probing depth and attachment level measurements were obtained prior to treatment and 9 months postsurgically prior to en bloc harvesting of the teeth and a measured amount of surrounding periodontium.¹⁶ The sites were reconstructed with autogenous bone grafts, and eventually endosseous implants were placed and restored with functional prostheses.

Micro-CT analysis

The specimens were scanned using a high-resolution micro-CT system (μCT 20, Scanco Medical) in multi-slice mode. Each 3D image data set consisted of approximately 400 micro-CT slice images (1,024 \times 1,024 pixels with 16-bit grey levels).

After measurements and reconstruction, a constrained 3D gaussian filter was used to partly suppress the noise in the stack of CT slices, ie, the discrete convolution of the

gaussian filter and the image data were computed only for limited finite filter supports. The specimen was scanned in high-resolution mode with an x-, y-, z- resolution around 20 μm . The voxel size was $15 \times 15 \times 15 \mu\text{m}^3$. Scanning time for the specimen was approximately 20 hours. Use of micro-CT provides an opportunity to quantify bone at this resolution with a geometric error around 0.3% (defined margin in the manufacturing process).

The following micro-CT parameters were evaluated in this study: (1) 2D and 3D structure of pre-existing bone and of newly regenerated bone in the vicinity of the root; (2) thickness and 3D shape of the periodontal space; (3) integration of new host bone with the particles of mineral collagen bone substitute; and (4) micro-CT suggestion of regeneration defined as adjacent new bone connected by a PDL space in relation to the notch on the root. These regions were qualitatively compared to the histologic samples.

Results

Clinical and histologic findings

Clinical evaluation at 9 months revealed a mean reduction in probing depth of 5.75 mm and a mean gain in attachment level of 5.25 mm.¹⁶ Histologic evaluation showed periodontal regeneration, with new cementum connected to new bone by a PDL at and coronal to the level of the calculus notch.¹⁶

Case	New bone + Bio-Oss (bone + graft)	Bio-Oss only	New bone only
1	71.03	21.17	49.86
2	33.03	8.38	24.65
3	58.45	14.07	44.38
4	35.93	7.52	28.41

Micro-CT findings

Qualitative analysis. The 3D reconstruction of the sequence of images from the micro-CT allowed analysis of the morphology of the entire specimen. The micro-CT examination was performed along three different planes: horizontal, vertical, and oblique.

Two different bone densities were observed, which were consistent with cortical bone and the trabeculae of cancellous bone. The particles of the mineral collagen bone substitute were visible and easily distinguished from host bone trabeculae, since the radiographic attenuation of grafted particles was different, but it was not possible to distinguish between the dentin and the cementum of the root. The structure of the endodontic canals and the dimensions and contour of the PDL space were evaluated.

In the area where the histologic analysis demonstrated a complete new attachment apparatus, a nor-

mal width of the periodontal space was observed, but a reduction in width was seen for localized areas of the periodontal space in the vicinity of the notch. There were no signs of root resorption or ankylosis, and graft particles were not in direct contact with the root surface.

A continuous shell of alveolar bundle bone (lamina dura) between 0.5 and 1 mm surrounded the root below the level of the calculus notch in all treated sites. An alveolus of identical dimension of newly formed bone surrounded the root in the treated area, restoring the anatomy of periodontal supporting bone. The newly formed bone was connected by bony trabeculae to the surrounding native bone.

Quantitative analysis. The percentage of anorganic bovine bone particles and the percentage of new bone were calculated within the treated defect site utilizing the micro-CT images with computer-assisted image analysis. The data are presented in Table 1.



Fig 1a Intrabony defects on the distal and mesial surfaces of the mandibular right first premolar. Note that the distal defect is a two/three-wall defect and the mesial defect is a one/two-wall defect.

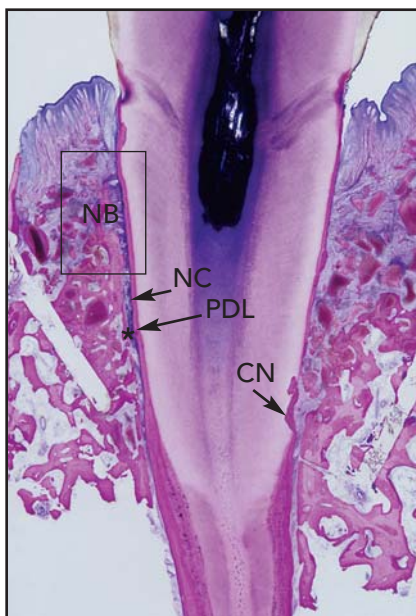


Fig 1b Histologic evaluation demonstrates a complete new attachment apparatus, with new cementum (NC), periodontal ligament (PDL), and alveolar bone (NB) adjacent to the root surface and coronal to the calculus notch (CN). The distal surface is on the left side with a more robust regenerative response than the mesial surface.

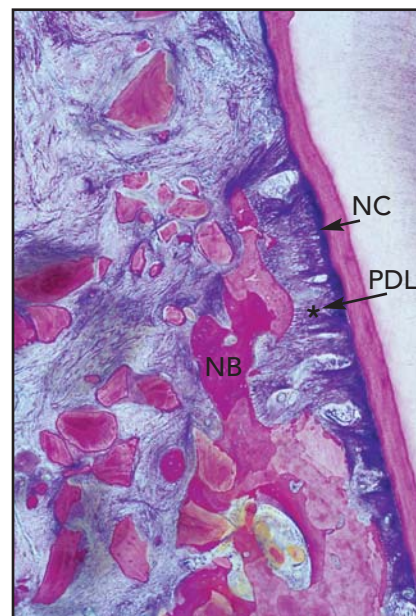


Fig 1c Higher-power view of the more coronal aspect of the distal defect shows regeneration with a vascular PDL connecting new alveolar bone to new cementum (NC). The anorganic bovine bone particles are surrounded by new bone (NB) and connected by bone trabeculae.

Case examples

Case 1. Case 1 addressed the proximal intrabony defects on a mandibular first premolar (Fig 1a). The defects were each treated with mineral collagen bone substitute alone. Postoperatively, the tissues

appeared clinically healthy. Radiographically, the area of the original defect exhibited increased radiopacity with no clear delineation between the grafted area and the native bone.¹⁶ Histologic evaluation provided evidence of periodontal regeneration with new cementum,

PDL, and alveolar bone coronal to the calculus notch (Figs 1b and 1c).¹⁶

Micro-CT evaluation of sections made at the level of the notch demonstrated restoration of the periodontium, with new bone present at the mesial and distal aspects of the treated tooth and no evidence

Fig 1d (right) Micro-CT transverse sections through central portion of defect (distal left and mesial right). The micro-CT image parallels the histologic views seen in Figs 1b and 1c. The mesial aspect is suggestive of new bone adjacent to the calculus notch with a PDL space of normal width. At the more coronal level, the PDL space widens and the graft material is less consolidated. The distal aspect is suggestive of regeneration, with the alveolar bone regenerated at the coronal aspect of the defect and a PDL space of normal width similar to the histologic view.

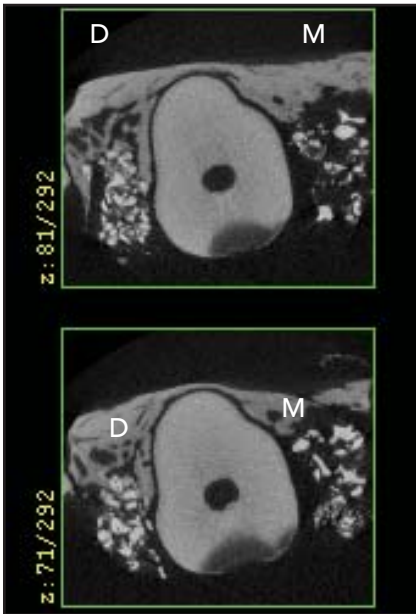
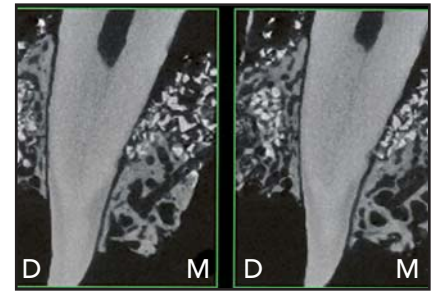


Fig 1e Micro-CT cross sections from the coronal portion of the defect. The distal (D) aspect demonstrates bone fill with a PDL space of normal width. The mesial (M) aspect has a widened PDL space and less opacity surrounding graft particles, suggestive of less regeneration in this region of the defect.

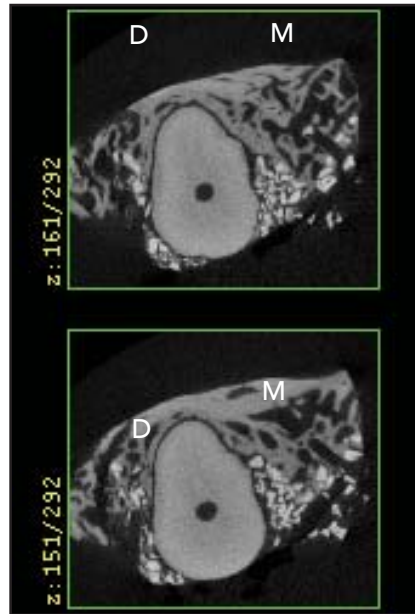


Fig 1f Micro-CT cross sections from the apical portion of the defect (D = distal; M = mesial). There is apparent bone fill for both the mesial and distal defects.

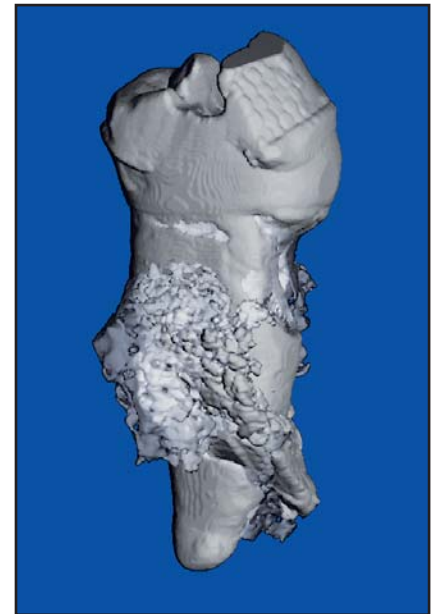


Fig 1g Micro-CT reformatted 3D image of distal aspect of mandibular first premolar, suggestive of bone fill of the defect in a supracrestal location.

of ankylosis (Fig 1d). The regenerative response at the coronal extent of the defect varied in a manner that was consistent with the number of bony walls present. The distal defect with three bony walls showed new supporting alveolar bone and a PDL of normal width, even in the

supracrestal location (Fig 1e). For the mesial aspect, however, the apical portion of the defect showed new bone formation and a normal PDL width consistent with regeneration, but the less-contained coronal region of the defect had less new bone formation with a connective

tissue attachment (Figs 1e to 1g). The distal sections showed new bone formation around many particles of anorganic bovine bone, demonstrating the osteoconductive properties of the material. New bone formation was measured to be 3.1 mm in this section.



Fig 2a (top left) A 7-mm one/two/three-wall intrabony defect located at the mesial aspect of the maxillary left canine. This defect was treated with Bio-Oss Collagen and a Bio-Gide membrane.

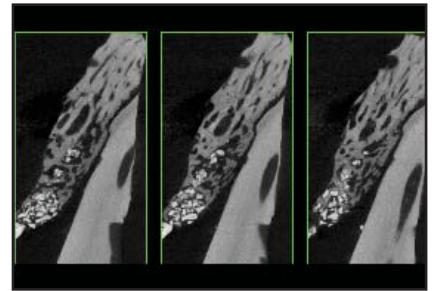
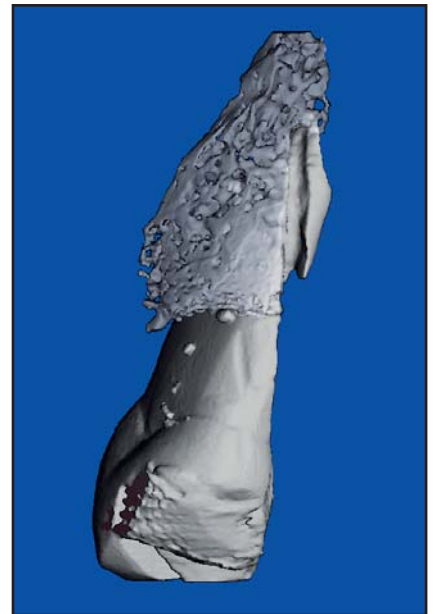


Fig 2b (bottom left) Histologic results show periodontal regeneration with new bone (NB), PDL (*), and new cementum (NC) adjacent to and coronal to the calculus notch (CN).



Fig 2c (top right) Transverse micro-CT sections, suggestive of periodontal regeneration. The micro-CT image corresponds closely with the section shown in Fig 2b.

Fig 2d (bottom right) Micro-CT 3D image of maxillary canine.



Case 2. The second case treated exhibited a 7-mm one/two/three-wall intrabony defect on the mesial aspect of a maxillary left canine (Fig 2a). This site, treated with mineral collagen bone substitute and protected by a Bio-Gide membrane, had an initial probing depth of 10 mm and a 9-month postoperative probing depth of 4 mm, for a reduction of 6 mm. Postsurgically, the tissues were clinically healthy, with a gain in attachment of 6 mm and no recession. Radiographically, the area of the original defect exhibited bone fill with

increased radiopacity and no clear delineation between the grafted area and the surrounding native bone.¹⁶ Histologic evaluation demonstrated periodontal regeneration coronal to the calculus notch, with new cementum, PDL, and alveolar bone (Fig 2b).

Micro-CT evaluation revealed 3 to 4 mm of new bone formed coronal to the calculus reference notch and a net reduction of the original defect. The width of the periodontal space was normal throughout the regenerated area, with no evidence of ankylosis. A coronal increase in

width of the periodontal space began about 0.5 to 1 mm apical to the location where histologic examination previously demonstrated the apical end of the junctional epithelium (Figs 2b and 2c).¹³

The microscopic anatomy of the newly formed alveolar process restored the anatomy of the lamina dura. Numerous trabeculae of new bone surrounded and connected the granules of anorganic bovine bone, demonstrating its osteoconductive properties.

Discussion

Micro-CT provides an opportunity for the very precise evaluation of hard tissues at various locations throughout a treated site. This non-destructive technique allows for detailed 2D and 3D analyses of hard tissues within the healing periodontium and preserves specimens for subsequent conventional histologic analysis. Results of the histologic observations for the cases used in this study have been published¹⁶ and are referenced as a control to compare the micro-CT observations. The micro-CT data demonstrated reconstruction of the periodontium adjacent to the calculus notch and coronal to it, with a normal PDL space in the regenerated area extending to a location that appeared to be consistent with previously demonstrated histologic evidence of the level of the junctional epithelium. In the region where regeneration was observed histologically, micro-CT demonstrated that newly formed bone filled the defect, allowing reconstruction of a significant dimension of new periodontal alveolar bone with a PDL space of normal dimensions.

The structure of the regenerated tissues was indistinguishable from the surrounding bone in the apical/notch area of the defect. Organized bone trabeculae surrounded particles of graft. Coronal to the region of the notch, graft particles were interspersed into a network of bone trabeculae. In more coronal micro-CT sections, coinciding with the widest portion of the defect containing fewer bony walls, graft particles were surrounded by connective tissue and connected by less organized trabeculae.

The micro-CT analysis allowed for 3D evaluation of the periodontal wound healing in relation to the number of osseous walls present for the defect. The bone shell was completely rebuilt, and the granules of biomaterial were connected into well-organized newly formed bony trabeculae in the three-wall portion of the defect. The width of the periodontal space between the root and alveolar bone appeared similar to that seen in healthy specimens. In the area where two bony walls were present, the bone shell was not restored completely, and granules of anorganic bovine bone were surrounded by new bone connected by less mature trabeculae. Where alveolar bone was restored, the PDL space appeared normal in width. In the area where only one bony wall was present, some of the particulate bone was surrounded by connective tissue, and only a few bridges of newly formed bone were present between grafted particles. As was observed histologically, micro-CT revealed new bone formation to be more extensive closest to the bony wall, while at the coronal periphery of the treated defect and closest to the tooth root, new bone formation

was not as robust. In these areas, the PDL space was wider.

For the two cases in which Bio-Oss Collagen was used as a barrier membrane to cover the "grafted" defect, micro-CT evaluation was consistent with histologic results, which demonstrated that supracrestal graft particles were embedded in dense connective tissue coronal to the level of the junctional epithelium.

Micro-CT analysis allows qualitative and quantitative 3D evaluation. This is a useful adjunct to current histologic techniques, as the data are collected prior to sectioning the specimen, when damage may occur or artifacts may be introduced. Micro-CT can be used independently to evaluate periodontal specimens or in combination with histologic evaluation.

References

1. Hancock EB. Regenerative procedures. In: *Proceedings of the World Workshop in Clinical Periodontics*, July 23–27, 1989. Chicago: The American Academy of Periodontology, 1989;VI:1–26.
2. Garrett S. Periodontal regeneration around natural teeth. *Ann Periodontol* 1996;1:621–666.
3. Bowers GM, Chadroff B, Carnevale R, et al. Histologic evaluation of new attachment apparatus formation in humans. Part III. *J Periodontol* 1989;60:683–693.
4. Bowers GM, Felton F, Middleton C, et al. Histologic comparison of regeneration in human intrabony defects when osteogenin is combined with demineralized freeze-dried bone allograft and with purified bovine collagen. *J Periodontol* 1991;62:690–702.
5. Hiatt WH, Schallhorn RG, Aaronain AJ. The induction of new bone and cementum formation: IV. Microscopic examination of the periodontium following human bone and marrow allograft, autograft, and non-graft periodontal regenerative procedures. *J Periodontol* 1978;49:495–512.
6. Stahl SS, Froum SJ, Kushner L. Healing responses of human intraosseous lesions following the use of debridement, grafting and citric acid root treatment. II. Clinical and histologic observations: One year post-surgery. *J Periodontol* 1983;54:325–338.
7. Mellonig JT. Human histologic evaluation of a bovine-derived bone xenograft in the treatment of periodontal osseous defects. *Int J Periodontics Restorative Dent* 2000;20:19–29.
8. Reynolds MA, Aichelmann-Reidy ME, Branch-Mays GL, Gunsolley JC. The efficacy of bone replacement grafts in the treatment of periodontal osseous defects. A systematic review. *Ann Periodontol* 2003;8:227–265.
9. Caton J, Zander H. Osseous repair of an intrabony defect without new attachment of connective tissue. *J Clin Periodontol* 1976;3:54–58.
10. Nevins ML, Camelo M, Nevins M, et al. Human histologic evaluation of bioactive ceramic in the treatment of periodontal osseous defects. *Int J Periodontics Restorative Dent* 2000;20:459–467.
11. Feldkamp LA, Goldstein SA, Parfitt AM, et al. The direct examination of three dimensional bone architecture in vitro by computed tomography. *J Bone Miner Res* 1989;4(1):3–11.
12. Ruegsegger P, Koller B, Muller R. A microtomographic system for the nondestructive evaluation of bone architecture. *Calcif Tiss Int* 1996;58(1):24–29.
13. Laib A, Ruegsegger P. Calibration of trabecular bone structure measurements of in vivo three-dimensional peripheral quantitative computed tomography with 28 micron-resolution microcomputed tomography. *Bone* 1999;24(1):35–39.
14. Ebbesen EN, Thomsen JS, Mosekilde L. Nondestructive determination of iliac crest cancellous bone strength by pQCT. *Bone* 1997 Dec;21(6):535–540.
15. Odgaard A. Three-dimensional methods for quantification of cancellous bone architecture. *Bone* 1997;20(4):315–328.
16. Nevins ML, Camelo M, Lynch SE, Schenk RK, et al. Evaluation of periodontal regeneration following grafting intrabony defects with Bio-Oss Collagen. *Int J Periodontics Restorative Dent* 2003;23:9–17.